ELSEVIER

Journal of Nuclear Materials 256 (1998) 69–77

journal of nuclear materials

Corrosion of annealed AISI 316 stainless steel in sodium environment

Vaidehi Ganesan [a,*], Vedaraman Ganesan [b]

[a] *Division for PIE and NDT, Indira Gandhi Centre for Atomic Research, Kalpakkam-603 102, India*
[b] *Materials Chemistry Division, Indira Gandhi Centre for Atomic Research, Kalpakkam-603 102, India*

Received 18 May 1995; accepted 16 February 1998

Abstract

Solution annealed AISI type 316 austenitic stainless steel specimens were exposed in static sodium at 773 and 873 K for durations ranging from 500 to 2000 h. The results, i.e, weight loss data, hardness values, carburisation, depletion rates, sigma phase formation from the ferrite layer, corrosion morphology, roughness values etc. are analysed and discussed in the paper. Corrosion data such as the weight loss/depleted layer thickness and microstructure of fully annealed stainless steel specimens at 773 and 873 K under static sodium conditions (present study) are comparable to those of 20% cold worked stainless steel type 316 specimens at temperatures 973 K and above under dynamic sodium conditions. Annealed specimens leach out at a faster rate than cold worked specimens exposed to sodium.

1. Introduction

Chemical interaction of hot sodium leading to solid state reactions in structural materials in contact with it have been investigated in great detail in order to arrive at the proper choice of materials for the construction of liquid metal cooled fast breeder reactor (LMFBR) circuits [1,2]. The choice of sodium metal as heat transfer medium stems from the merits of its physical properties such as high boiling point, low vapour pressure, high thermal conductivity and good heat transfer property in addition to favorable chemical and nuclear properties. Owing to this choice, corrosion of materials in sodium environment assumes great importance. The chemical compatibility of sodium with structural materials is generally good when sodium is in its pure state. However, presence of impurity elements in liquid sodium leads to corrosion. The interaction and compatibility of sodium with AISI type 316 stainless steels have been extensively studied [3–10]. In this paper, corrosion results obtained under static conditions are presented. The observed corrosion data such as weight loss, depleted layer formation, changes in microstructures etc. of annealed specimens vis-à-vis cold worked specimens under dynamic conditions are discussed.

2. Sodium corrosion

The corrosion by liquid metals such as sodium, is quite different from that encountered in aqueous systems and needs detailed understanding for successful design and operation of LMFBRs. Corrosion is degradation of materials which may lead to failure in extreme circumstances. Corrosion problems are encountered in chemical, thermal and nuclear plants. Owing to the fact that liquid sodium is used as heat transfer medium in LMFBRs, corrosion of structural materials, predominantly austenitic stainless steels, in sodium environment assumes significance.

Corrosion in sodium environment is influenced by many interrelated factors. Factors that influence sodium corrosion are the base composition and thermo-physical condition of the material, temperature, oxygen and carbon content of sodium, material position in relation to the heat input zone, sodium axial heating rate, mechan-

* Corresponding author. E-mail: vaidehi@igcar.ernet.in.

0022-3115/98/$19.00
PII: S0022-3115(98)00041-5

ical stress in the material, sodium velocity, poly-thermal nature of the system, exposure time and dissimilar materials in contact with sodium [3].

Two predominant corrosion processes applicable to austenitic stainless steels in liquid sodium are selective leaching and steady state corrosion [4]. Although stainless steel is generally compatible with sodium in pure state, presence of oxygen in low levels causes selective leaching of chromium by forming the ternary $NaCrO_2$ phase. The ferritisation takes place during the initial period of exposure (lasting for thousands of hours) and the steady state corrosion becomes the predominant cause of degradation beyond this incubation time, thus governing the corrosion rate of austenitic stainless steels for long term behaviour. Influence of carbon on weight change is dictated by carbon activity in sodium in relation to that in stainless steel, leading to carburisation or decarburisation situation. However, the effect of carbon on weight change is very small compared to weight loss associated with selective leaching of chromium. The weight loss due to sodium exposure consists of two components, the weight loss due to ferritisation and that due to steady state corrosion. The weight loss due to steady state corrosion can be correlated to volume diffusion coefficients. Once the ferrite layer is formed, the growth of ferrite layer is controlled by diffusion parameters. According to Williams and Faulkner [12], diffusion data from diffusion couples are considered to be more realistic than those obtained from tracer work for the process of predicting diffusion controlled corrosion behaviour in austenitic stainless steel systems. It is evident that simple boundary conditions in diffusion can be used to understand the corrosion behaviour in stainless steel/sodium (SS/Na) system [11,23].

3. Experimental

Austenitic AISI type 316 stainless steel samples were exposed in static sodium at 773 and 873 K for 500–2000 h durations in steps of 500 h. The sodium, prior to corrosion run, was gettered using vanadium foil at 773 K for 24 h. The nominal oxygen and carbon levels in sodium throughout the test were 1–2 ppm and 10–12 ppm, respectively. The chemical composition of the materials used are presented in Table 1. The specimens were in annealed condition (1323 K for $\frac{1}{2}$ h) with an average grain size of 130 ± 5 μm. The specimens were polished upto coarse diamond polishing on both sides. The schematic diagram of the experimental vessel is shown in Fig. 1. About 20 g of sodium was loaded into this vessel, the handling of sodium being performed inside an argon atmosphere glove box. Stainless steel specimens of dimensions 15 × 10 × 2 mm were suspended from the top of the vessel and kept immersed in sodium. The experimental vessel was secured leak-tight using knife-edge flanges employing annealed copper gasket. The micro-hardness of the samples was measured by applying 50 g load on the sodium exposed surface. The carbon profiles of the sodium exposed specimens were obtained by secondary ions mass spectrometry (SIMS) analysis. The microstructures of the sodium exposed surfaces and the cross-sections were characterised using scanning electron microscopy (SEM).

Table 1
Chemical composition of materials

Element	AISI type 316 L SS	Sodium (ppm)
C	0.052	10–12
Si	0.505	–
Mn	1.509	–
Ni	15.068	–
Cr	15.051	–
Mo	2.248	–
S	0.003	–
P	0.011	–
Fe	Balance	–
Co	0.015	–
Ti	0.315	–
Ta + Nb	0.020	–
N	0.007	–
B	0.001	–
O	–	1–2

Values in wt% unless stated otherwise.

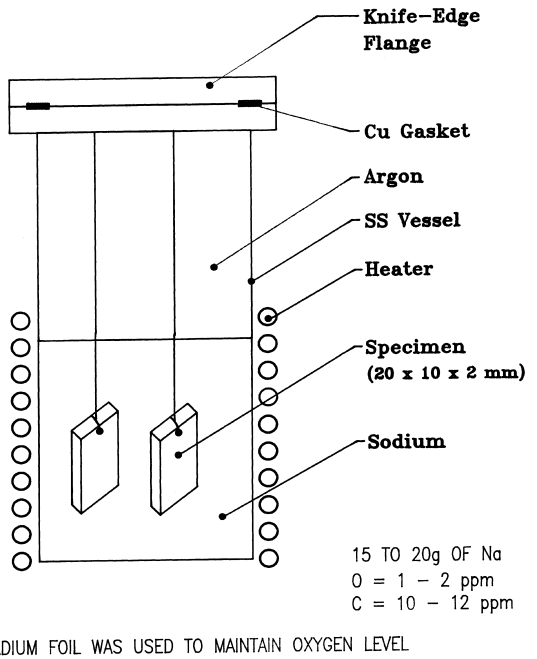

Fig. 1. Static sodium experimental setup.

4. Results

The micro-hardness measurements showed an increase in hardness values from 150 ± 7 VHN in the annealed specimens to 250 ± 10 VHN after sodium exposure of 2000 h at 873 K. The increase in micro-hardness on the surface is attributed to carbon pick up in stainless steel owing to carburisation and this was established qualitatively by SIMS analysis as shown in Fig. 2. The figure shows a sputter depth of about 0.55 μm for specimens exposed at 873 K for 2000 h. The carbon profile taken is from bulk and not through grain boundary. There is carbon pickup up to about 0.4 μm from the surface of the specimen. The typical depleted layer in sodium exposed specimen, shown in Fig. 3(a) is of 5–7 μm width for specimens exposed at 773 K for 500 h and 10 μm for those exposed at 873 K for 1000 h. In the specimen exposed at 873 K for 2000 h, the depleted layer width is of the order of 15 μm. The layer thickness increases with increase in temperature and time of exposure. This layer is depleted in chromium and nickel as found by the energy dispersive analysis of X-rays (EDAX). The results are shown in Figs. 3(b) and 3(c).

The weight loss data obtained after sodium exposure at 773 and 873 K are presented in Table 2. There is a general increase in the weight loss with temperature and duration of exposure. The slight decrease in weight loss for specimens exposed at 773 for 1000 h compared to that at 773 K for 500 h may be attributed to the change in mechanism from selective leaching (ferrite formation) to steady state corrosion (ferrite layer growth). The effect of change in mechanism on mass loss is pronounced at lower temperatures and not so at higher temperatures where the increased steady state corrosion rate outweighs the effect due to mechanism change.

The precipitates depleted in chromium and nickel on the surface were observed which are shown in Fig. 4(a). Fig. 4(b) shows the corrosion resistant nodes seen clearly on the surfaces of the samples exposed at 873 K for 514 h. These nodes disappear or are washed away in sodium (even in static condition) at higher temperature and/or duration of exposure as shown in Fig. 5. The transformation of ferrite from austenite matrix and the appearance of sigma-phase from ferrite is also established experimentally using XRD technique and the results are shown in Table 3. The roughness values were measured with an accuracy of ±0.1 μm, using a surf test machine (conventional profilometer) of Japan make Mitutoyo model Surftest-211. The profilometer gives an average value of 5 points from a linear length of 4 mm. In the pre-exposed condition, the surface roughness values were 0.42 μm. In minimum (773 K for 500 h) and maximum (873 K for 2000 h) exposure conditions, the values were 0.56 and 1.38 μm, respectively (Table 4). The calculated depletion rates based on simple boundary conditions, $x^2 = 4Dt$ (composition independent D values), are presented in Table 5.

5. Discussion

The recommended grain size of austenitic stainless steel is 50 μm for reactor applications. The smaller grain size is normally achieved with 20% cold working. Annealed specimens of grain size 125–130 μm are used in the present study. This is to compare the results obtained using annealed specimens with those of cold worked specimens exposed in sodium taken from literature. Moreover, application of simple models of diffusion to obtain the leaching rates of major elements are emphasised.

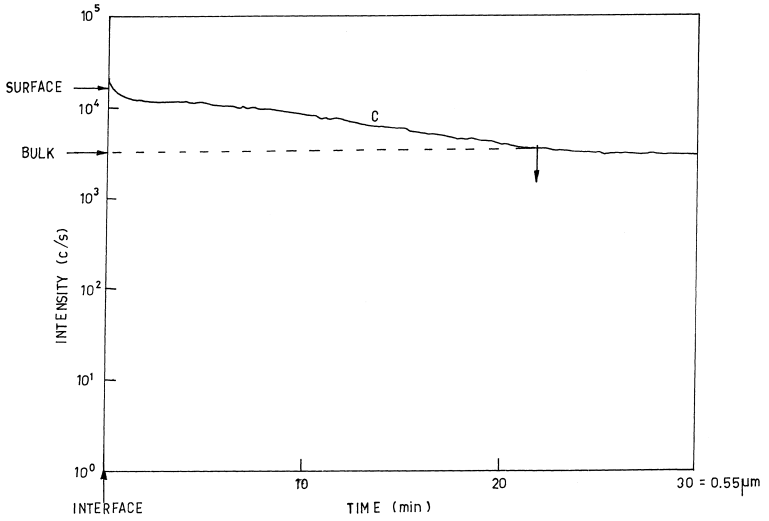

Fig. 2. Carbon profile vs. sputter depth by SIMS analysis in AISI type 316 stainless steel exposed to sodium at 873 K for 2000 h.

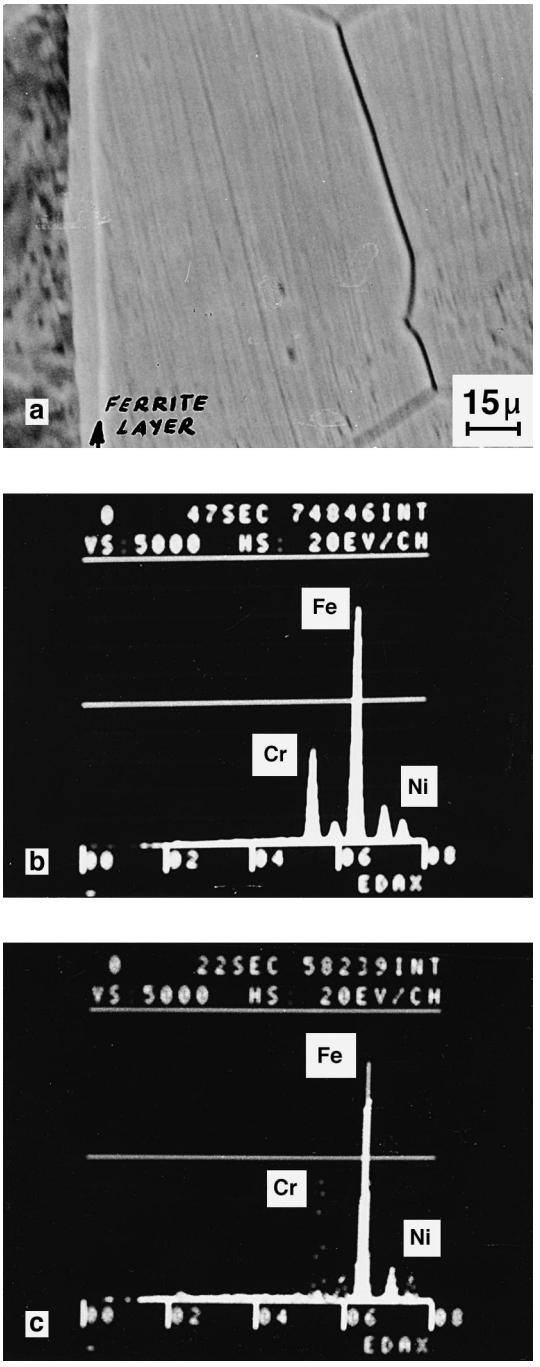

Fig. 3. (a) SEM micrograph of cross-section showing Cr and Ni depleted layer at 873 K–2000 h. (b) EDAX analysis of austenite matrix. (c) EDAX analysis of Cr and Ni depletion as shown in morphology (a).

The corrosion rates of austenitic stainless steels, under otherwise identical conditions, are significantly influenced by dissolved oxygen in liquid sodium. This can be seen from the expression derived by Thorley and Tyzack [10] relating oxygen content in sodium to corrosion rate of austenitic stainless steels under high velocity conditions. The expression for corrosion is given below.

$$\log S = 2.44 + 1.5 \log(O) - 18\,000/(2.3\,\mathrm{R}T),$$

where S is the rate of metal loss (mil/yr) (units as used in the model), O the oxygen concentration (ppm) and T the

Table 2
Weight loss data in 316 SS/Na system

773 K		873 K	
Duration (h)	Wt. loss (mg cm^{-2})	Duration (h)	Wt. loss (mg cm^{-2})
500	0.0325	500	0.025
1000	0.025	1000	0.213
1540	0.1325	1490	0.285
2000	0.285	2013	0.575

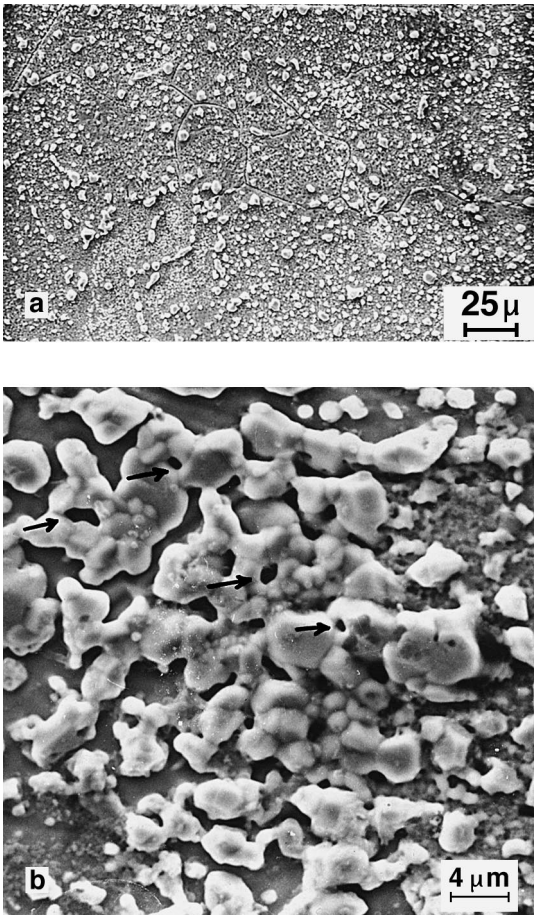

Fig. 4. (a) Surface morphology, Cr and Ni depleted precipitates, ferritisation at 773 K–500 h; roughness Ra = 0.56 μm. (b) Surface morphology, corrosion resistant nodes formation at 873 K–514 h; roughness Ra = 0.76 μm.

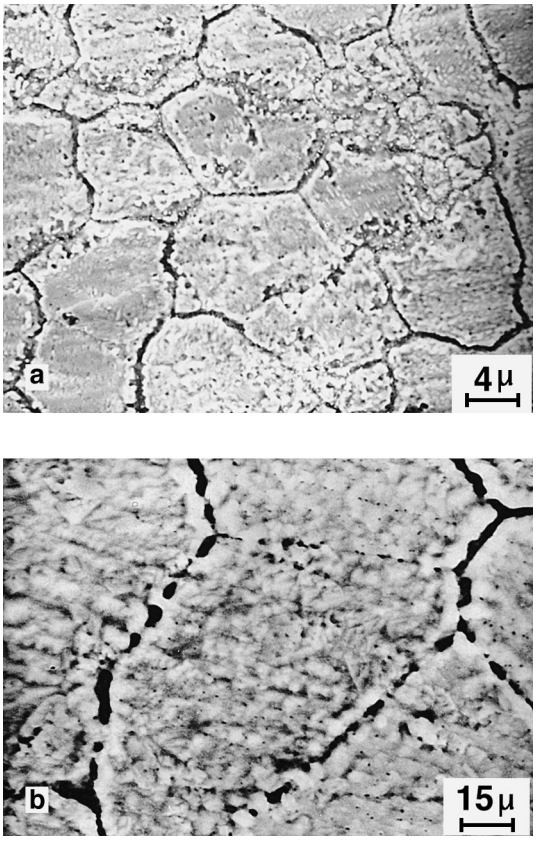

Fig. 5. Surface morphologies at 773 K–2000 h and 873 K–2000 h. (a) Roughness Ra = 1.24 μm; (b) Roughness Ra = 1.38 μm. Nodes washed away during prolonged sodium exposure.

temperature of sodium (K). According to Koltser [4], the steady state corrosion of austenitic stainless steel in liquid sodium containing up to 8 ppm of oxygen is linearly dependent on the oxygen level as given by the relation

$$I = K + C(O),$$

where (O) is the oxygen content in sodium, K the rate constant for dissolution of metallic elements in sodium and C the rate constant for the reaction of metallic elements with oxygen. The corrosion rate I is expressed in mg cm^{-2} yr^{-1}. Values of K and C at 923 and 973 K as a function of downstream position for oxygen contents ranging from 1 to 8 ppm have been reported in this work. The velocity of sodium was 6 m s^{-1} with samples kept at different downstream positions [4].

Borgstedt [5] has employed annealed specimens in the temperature range of 873–973 K in experimental loop with sodium velocity of 5 m s^{-1}. The oxygen level was maintained between 3.5 and 8.9 ppm and the carbon content was in the range of 70–180 ppb. The activation

Table 3
X-ray diffraction data in 316 SS/Na system

Temperature–time	2θ	Sin θ	d	Plane
773 K–500 h	43.8	0.37	2.08	$(111)_\gamma$
	44.8	0.38	2.08	$(011)_\alpha$
	51.0	0.43	1.79	$(200)_\gamma$
	74.8	0.61	1.26	$(220)_\gamma$
773 K–1000 h	28.7	0.25	3.08	$(030)_\sigma$
	43.8	0.37	2.08	$(111)_\gamma$
	50.8	0.43	1.79	$(200)_\gamma$
	74.8	0.61	1.26	$(220)_\gamma$
773 K–2000 h	28.8	0.25	3.097	$(030)_\sigma$
	43.8	0.37	2.08	$(111)_\gamma$
	44.8	0.38	2.03	$(011)_\alpha$
	51.0	0.43	1.79	$(200)_\gamma$
	74.8	0.61	1.26	$(220)_\gamma$

θ – Bragg angle; d – interplanar spacing (Å); Target – CuKα; $\lambda = 1.54056$ Å.

Table 4
Roughness values of specimens exposed to sodium

Sl. no.	Temperature (K)	Time (h)	Roughness (μm)
1	773	500	0.56
2	773	1000	0.75
3	773	1540	0.91
4	773	2000	1.24
5	873	1000	0.91
6	873	2000	1.38

Table 5
Comparison of leaching rates in SS/Na system with literature data

Parameter	Static sodium (this work)		Dynamic sodium [9]	Dynamic sodium [9]
1. Specimen condition	Annealed (grain size 130 ± 5 μm)	Annealed (grain size 130 ± 5 μm)	20% cold worked	20% cold worked
2. Temperature (K)	773	873	1028	973
3. Time (h)	500–2000	500–2000	2500	8000
4. Layer Width (μm)	6–8	7–15	18–20	27
5. Leaching rate (m^2 s^{-1})				
Initial	0.050×10^{-16}	0.068×10^{-16}	0.09×10^{-16}	0.063×10^{-16}
Steady state	0.022×10^{-16}	0.078×10^{-16}	0.11×10^{-16}	

energy for sodium corrosion in their studies was found to vary from 175.9 to 75.7 kJ mol^{-1}. Analysing the above data, it can be derived that the wide variation in the activation energy is due to decrease in activation energy for corrosion processes involving increasing oxygen content in sodium.

Carburisation of specimens was observed in the present study as revealed by SIMS profiles shown in Fig. 2. Carburisation has also been reported in steels 1.4301 and 1.4948 (steels similar to AISI type 316) and in Inconel 800 [5]. According to the study cited in Ref. [5], corrosion rates were not proportional to the nickel content of the alloys. In the carburised areas, $M_{23}C_6$ and M_7C_3 type carbides were reported which could be in/near ferrite layer. The carbides observed in the present work are yet to be analysed and hence are not discussed here.

Comparison of weight loss data reported by Borgstedt [5] and that obtained in the present work for specimens at 873 K exposed for longer duration reveals that the weight loss of annealed specimens under static conditions is less compared to that under dynamic conditions (Table 6). Temperature, duration, material, carbon and oxygen level in sodium and the specimen condition (annealed) are comparable in both the experiments. In general, when other conditions remain same, weight loss in dynamic sodium would be higher than that in static sodium. The macro mass transfer from bulk (solid) to liquid which is in flowing condition, is comparatively higher than the mass transfer occurring in static condition. The driving force for this mass transfer is the boundary layer diffusion.

Suzuki and Mutoh [6,7] have reported corrosion studies with cold worked AISI type 316 stainless steel under dynamic sodium conditions with oxygen content of 1–2 ppm and sodium velocity of 4 m s^{-1}. The weight losses reported by them are found to be less compared to that reported by Borgstedt for annealed AISI type 316 stainless steel specimens exposed in sodium under dynamic conditions (Table 7).

The compositions of the samples used in the above studies are nearly the same and the experimental conditions such as the oxygen content and the sodium velocity are comparable. Annealed specimens show higher weight loss than cold worked specimens when the other conditions remain same.

Comparison of the weight loss data of Suzuki and Mutoh [6,7] with the present results reveals that the cold worked specimens under dynamic sodium conditions show lower weight losses as compared to annealed specimens under static sodium conditions at 873 K (Table 8).

Thus from the analysis of the weight loss data, we draw the conclusion that the 20% cold worked material exhibits lower weight loss compared to annealed specimens in static or dynamic conditions at 873 and 973 K. The major contribution for weight loss data is due to steady state corrosion. Steady state corrosion advances with ferrite layer formation. It is observed in these experiments that the depleted layer can form easily in annealed specimens (grain size = 130 ± 5 μm). In cold worked material, selective leaching and diffusion in the later stages are slow leading to slower rate of transformation of ferrite and ferrite layer formation.

Borgstedt has compared his experimental results [5] with different empirical models by Weeks and Isaacs [13], Thorley and Tyzack [10], Kolster [14] and certain other models mentioned in his work [5] and recommends Thorley and Tyzack's model [10], taking into account high temperature, long time of exposure with high sodium velocity, as the most suitable model for extrapolation and application of experimental results to predict the life time of structural materials in nuclear power plants. The general corrosion equation proposed by Thorley and Tyzack [10] is given earlier.

Shiels et al. [8] have reported wall thinning of 12–14 μm for AISI type 316 stainless steel after 8000 h of exposure at 973 K in sodium containing 1 ppm of oxygen. This wall thinning is less compared to that for materials like PE16 and Inconel. Stainless steel AISI type 330 has the maximum wall thinning of 45 μm for the same experimental conditions mentioned above. In their experiments also, they have observed Fe–Mo nodes similar

Table 7
Comparison of weight loss data

Temperature (K)	Cold worked [6,7] (g m^{-2})	Annealed [5] (g m^{-2})	Time (h)
873	2.0	5.0	1500
873	2.5	8–9	2000
973	11	20	1000
973	17	35	2000
973	22	45	3000
973	27	50	4000

Table 6
Comparison of weight loss data

Time (h)	Static, annealed (present work) (g m^{-2})	Dynamic, annealed [5] (g m^{-2})
1500	2.85	5.0
2000	5.75	8–9

Table 8
Comparison of weight loss data

Cold worked (dynamic) [6,7] (g m^{-2})	Annealed (static, present work) (g m^{-2})	Time (h)
2.0	2.85	1000
2.5	5.75	2000

to that observed in the present work (Fig. 4 (b)) which modify themselves finally to coral like structure.

Loss in wall thickness calculated from weight loss data are comparable with the ferrite layer thickness. The cumulative or total damage is defined as the sum of wall thinning, degraded zone and inter-granular attack. The oxygen content of sodium in their experiments was 1–2 ppm and the velocity of sodium was 4.8–6.0 m s^{-1}. Total damage for cold worked AISI type 316 stainless steel after 8000 h of exposure at 973 K was 27 μm. The surface composition of the above specimens changed to 95% Fe, 2% Cr and <1% Ni after 10 000 h of exposure at 973 K. Alloys without molybdenum develop porosity. Corrosion rate was not a simple function of nickel content. Nickel was a prime contributor for corrosion of steels (solid solution alloys) in sodium.

We have already mentioned that Fe–Mo corrosion resistant nodes are formed on specimens exposed at 873 K for 500 and 1000 h and on specimens exposed at 773 K for 1500 h. Molybdenum plays an important role in forming corrosion resistant nodes. We can say the best corrosion resistant alloys in sodium are those with high molybdenum content or pure molybdenum itself. In the literature [15], molybdenum coating of vanadium by chemical vapor deposition technique was used to improve and to protect pure vanadium and vanadium alloy from sodium corrosion. In order to eliminate the influence of structural material on corrosion rate of stainless steel, Kolster and Bos [16] have studied sodium corrosion in molybdenum loop system.

The leaching rate of elements is calculated using the simple diffusion model $x^2 = 4Dt$, taking into account the total damage region of 27 μm at 973 K for 8000 h of exposure. The leaching rate is 0.063×10^{-16} m^2 s^{-1}. This value is found to be comparable to that in the initial stage of leaching obtained in the present study for samples exposed at 773 and 873 K for 500 h (0.05×10^{-16} and 0.068×10^{-16} m^2 s^{-1}) as given in Table 5.

These leaching rates can be compared with the tracer diffusivities of chromium and nickel in alpha or gamma phase [17–19]. The leaching rate calculated from the depleted layer is about 10^3 times greater than the tracer diffusivities of chromium and nickel in alpha or gamma phase. Extrapolation of the results of Bowen and Leak [17] for chromium diffusion (tracer) at 773 and 873 K in stainless steel 316 leads to diffusivity values of the order of 10^{-20} m^{-2} s^{-1}. Experimental results for diffusion of chromium in stainless steel measured by Matzke and Pickering [18] show chromium diffusivity value of 3×10^{-20} m^2 s^{-1} in stainless steel at 953 K. Extrapolated tracer diffusivity values of chromium and nickel by Assasa and Guiraldenq [19] are of the order of 10^{-23}, 10^{-21} and 10^{-19} m^2 s^{-1} at 773, 873 and 973 K respectively. This is lower than the present leaching rate of $\sim 10^{-16}$ m^2 s^{-1} at 773 and 873 K.

The composition profiles reported by Olander [9] for cold worked AISI type 316 specimens exposed under dynamic sodium conditions at 1028 K for 2500 h show depleted layer width of 18 to 20 μm. The leaching rate determined using composition independent models is 0.09×10^{-16} m^2 s^{-1}. This is comparable to the leaching rate (0.078×10^{-16} m^2 s^{-1}) obtained in the present study for annealed AISI type 316 specimens exposed at 873 K for 2000 h under static sodium conditions as shown in Table 5. This is consistent with the earlier conclusion that annealed AISI type 316 specimens leach at a faster rate and exhibit higher mass loss compared to 20% cold worked material in static or dynamic sodium conditions.

Single inter-diffusion coefficient is sufficient to explain the diffusion behaviour in binary systems [20]. Diffusion in ternary and multicomponent systems are quite different from that in binary systems [21–23]. The diffusion coefficients in multicomponent systems can be computed using the methods outlined by Kirkaldy [11] and Rooper and Whittle [24]. According to Manning [25], the diffusion coefficient in a multicomponent system can be described as an n^2 matrix where n is number of elements in the system. In the present study, simple model of diffusion, $x^2 = 4Dt$ is applied to calculate the leaching rate of chromium and nickel in austenitic stainless steel exposed to sodium. The composition profiles obtained using electron probe micro analyser in SS 316/Na system [9] suggest that these profiles can be treated as multicomponent diffusion profiles and the rate at which the major elements of stainless steel leach or diffuse out in sodium environment, can be established using Boltzmann–Matano method [23]. Based on the arguments presented by Kirkaldy [11,21], Rooper and Whittle [24] and Manning [25], multicomponent diffusion concepts were emphasised in earlier work [23].

The appearance of sigma phase in annealed AISI 316 stainless steel after sodium exposure (present results) is consistent with the observations of Miller et al. [26]. According to this study [26], sigma phase is the dominant precipitate in annealed Type 316 SS after sodium exposure. Anantamula [27] also has predicted sigma phase formation in AISI type stainless steel 316 clad tubes. The increase in the roughness values (Table 4), with sodium exposure and the possible correlation with corrosion is discussed by Thorley and Tyzack [10]. The surface roughness is attributed to the leaching of major elements from the surface and carburisation of the surface due to carbon present in sodium.

There is an interesting observation on the surface of sodium exposed specimens as shown in Figs. 5(a) and 5(b). It is interesting to observe diffusion induced recrystallization (DIR) on the surface of sodium exposed specimens. The grain size of the specimens prior to sodium exposure was 130 ± 5 μm. There is no evidence of recrystallisation and the grain size was greater than 130

μm for specimens exposed at 773 K for 500 h as shown in Fig. 4(a). The specimens exposed at 773 and 873 K for 2000 h each show clear evidence of DIR. The grain sizes are approximately, 25 ± 5 μm at 773 K–2000 h and 75 ± 5 μm at 873 K–2000 h, respectively. DIR and diffusion induced grain boundary migration (DIGM) have been observed in many systems [28–33].

DIR and DIGM are recently recognised low temperature phenomena which lead to unexpected grain boundary migration and vastly enhanced mass transport [28–31]. Recently it has been reported that DIGM is observed in more than 40 alloy systems [32]. DIGM has been observed in SS 316/Fe system with precipitation [22] and DIR has been observed in Fe–Ni system [33] without precipitation.

6. Conclusions

1. Weight loss of annealed specimens in static sodium environment (present study) is less compared to that in dynamic sodium under otherwise similar conditions.
2. The weight loss of 20% cold worked stainless steel type 316 specimens is less compared to that of annealed specimens under static (present study) or dynamic conditions at 873 and 973 K.
3. Corrosion data such as the weight loss/depleted layer and microstructure of fully annealed stainless steel specimens at 773 and 873 K under static sodium conditions (present study) are comparable to those of 20% cold worked stainless steel type 316 specimens at temperatures 973 K and above under dynamic sodium conditions.
4. Sigma phase easily nucleates near the leached zone in the annealed specimens exposed to sodium.
5. Fe–Mo corrosion resistant nodes are formed on specimens exposed at 873 K for 500 and 1000 h and on specimens exposed at 773 K for 1500 h. Molybdenum plays an important role in forming corrosion resistant nodes. It may be relevant to note that addition of Mo to stainless steels enhances the resistance to void swelling. The most corrosion resistant alloys in sodium are those with high molybdenum content and pure molybdenum.
6. DIR has been observed in specimens exposed to sodium at 773 K for 2000 h and at 873 K for 2000 h.

Acknowledgements

The authors wish to thank Ms M. Radhika for SEM micrographs and Mr T. Jayakumar for useful discussions. They also wish to thank Dr G. Periaswami, Head, Materials Chemistry Division, Dr Baldev Raj, Director, Metallurgy and Materials Group and Dr P. Rodriguez, Director, IGCAR for constant encouragement and support.

References

[1] I.R. Cameron, Nuclear Fission Reactors, Plenum, New York, 1982, p. 282.
[2] H.U. Borgstedt, C.K. Mathews, in: Applied Chemistry of Alkali Metals, Plenum, New York, 1987.
[3] A.R. Keeton, C. Bagnall, in: J.M. Dahlke (Ed.), Proceedings of the Second International Conference on Liquid Metal Technology in Energy Production, CONF-800401-P1, Richland, Washington, DC, 1980, p. 7–18.
[4] Kolster, in: J.M. Dahlke (Ed.), Proceedings of the Second International Conference on Liquid Metal Technology in Energy Production, CONF-800401-P1, Richland, Washington, DC, 1980, p. 7–53.
[5] H.U. Borgstedt, in: J.M. Dahlke (Ed.), Proceedings of the Second International Conference on Liquid Metal Technology in Energy Production, CONF-800401-P1, Richland, Washington, DC, 1980, p. 7–1.
[6] T. Suzuki, I. Mutoh, J. Nucl. Mater. 139 (1986) 97.
[7] T. Suzuki, I. Mutoh, J. Nucl. Mater. 140 (1986) 56.
[8] S.A. Shiels, C. Bagnal, A.R. Keeton, R.E. Witkowski, R.P. Anantatmula, in: J.M. Dahlke (Ed.), Proceedings of the Second International Conference on Liquid Metal Technology in Energy Production, CONF-800401-P1, Richland, Washington, DC, 1980, p. 7–11.
[9] D.R. Olander, Fundamental aspects of nuclear reactor fuel elements, USAEC Report TID-26711-P1, 1976, p. 361.
[10] A.W. Thorley, C. Tyzack, Liquid Alkali Metals, BNES, London, 1973, p. 257.
[11] J.S. Kirkaldy, Can. J. Phys. 35 (1957) 435.
[12] P.I. Williams, R.G. Faulkner, J. Mater. Sci. 22 (1987) 3537.
[13] J.R. Weeks, H.S. Isaacs, Adv. Corros. Sci. Tech. 3 (1973) 1.
[14] B.H. Kolster, in: Seventh International Congress on Metallic Corrosion, Rio de Janeiro, Brazil, 1978.
[15] M. Fukutomi, M. Okada, R. Watanabe, J. Less Common Met. 48 (1) (1976) 65.
[16] B.H. Kolster, L. Bos, in: Proceedings of the Third International Conference on Liquid Metal Engineering and Technology, vol. 1, Oxford, April 1984, The British Nuclear Energy Society, London, 1984, p. 9.
[17] A.W. Bowen, C.M. Leak, Metall. Trans. 1 (1969) 1695.
[18] H. Matzke, Pickering, J. Nucl. Sci. Tech. 20 (3) (1985) 237.
[19] W. Assasa, P. Guiraldenq, Met. Sci. 12 (1978) 123.
[20] Vaidehi Ganesan, V. Seetharaman, V.S. Raghunathan, Mater. Lett. 12 (4A) (1984) 257.
[21] J.S. Kirkaldy, Adv. Mater. Res. 4 (1970) 55.
[22] Vaidehi Ganesan, V. Seetharaman, V.S. Raghunathan, J. Nucl. Mater. 118 (1983) 313.
[23] Vaidehi Ganesan, in: International Conference on Physical Metallurgy, Bombay, India, ICPM-94, March 9–12, 1994, Trans. Indian Inst. Met. 45 (1995) 253.
[24] G.W. Rooper, D.P. Whittle, Scripta Metall. 8 (1974) 1357.
[25] J.R. Manning, Metall. Trans. 1 (1970) 499.
[26] R.L. Miller et al., in: Proceedings of the International Metallographic Society, 1970.

[27] R.P. Anantamula, J. Nucl. Mater. 125 (1984) 170.
[28] F.J.A. Den Broeder, Acta Metall. 20 (1972) 319.
[29] M. Hillert, G.R. Purdy, Acta Metall. 26 (1978) 333.
[30] R.W. Baluffi, J.W. Cahn, Acta Metall. 29 (1981) 493.
[31] P.G. Shewmon, Acta Metall. 29 (1981) 1567.
[32] Z. Guan, G. Liu, J. Du, Acta Metall. 41 (1993) 1293.
[33] Vaidehi Ganesan, in: Proceedings of the International Conference on Diffusion in Materials, Nordkirchen, Germany, DIMAT-96, August 5–9, 1996, Diffusion and Defect Forum, Science Technology, Switzerland, vol. 1583, 1997, p. 143.